J. Membrane Biol. 126, 171–181 (1992)

The Journal of
Membrane Biology


# Inwardly Rectifying Potassium Current in Rabbit Osteoclasts: A Whole-Cell and Single-Channel Study

Melanie E.M. Kelly†, S. Jeffrey Dixon†‡, and Stephen M. Sims†
†Department of Physiology and ‡Division of Oral Biology, University of Western Ontario, London, Ontario, Canada N6A 5C1

**Summary.** Ionic conductances of rabbit osteoclasts were investigated using both whole-cell and cell-attached configurations of the patch-clamp recording technique. The predominant conductance found in these cells was an inwardly rectifying $K^+$ conductance. Whole-cell currents showed an N-shaped current-voltage (*I-V*) relation with inward current activated at potentials negative to $E_K$. When external $K^+$ was varied, *I-V* curves shifted 53 mV/10-fold change in $[K^+]_{out}$, as predicted for a $K^+$-selective channel. Inward current was blocked by $Ba^{2+}$ and showed a time-dependent decline at negative potentials, which was reduced in $Na^+$-free external solution. Inward single-channel currents were recorded in the cell-attached configuration. Single-channel currents were identified as inward-rectifier $K^+$ channels based on the following observations: (i) Unitary *I-V* relations rectified, with only inward current resolved. (ii) Unitary conductance ($\gamma$) was 31 pS when recorded in the cell-attached configuration with 140 mM $K^+$ in the pipette and was found to be dependent on $[K^+]$. (iii) Addition of $Ba^{2+}$ to the pipette solution abolished single-channel events. We conclude that rabbit osteoclasts possess inwardly rectifying $K^+$ channels which give rise to the inward current recorded at negative potentials in the whole-cell configuration. This inwardly rectifying $K^+$ current may be responsible for setting the resting membrane potential and for dissipating electrical potential differences which arise from electrogenic transport of protons across the osteoclast ruffled border.

**Key Words** $K^+$ channel · inward rectification · patch clamp

## Introduction

Osteoclasts are large multinucleated cells with the unique ability to mediate extracellular resorption of bone. An active osteoclast adheres tightly to the bone surface forming an extracellular compartment, the resorption lacuna, between the cell membrane and the bone (Vaes, 1988). Osteoclasts transport protons and secrete lysosomal enzymes across a specialized membrane, "the ruffled border," into this confined compartment. It is within this acidic microenvironment that bone mineral is dissolved and the organic matrix is digested (Baron et al., 1985; Blair et al., 1986). Recent evidence has demonstrated that acidification of the resorption lacuna is mediated by the vacuolar class of ATP-driven proton pump ($H^+$-ATPase), located in the osteoclast ruffled border (Blair et al., 1989; Bekker & Gay, 1990; Väänänen et al., 1990). Studies of the $H^+$-ATPase in osteoclasts and other cell types has demonstrated that the presence of appropriate membrane ionic fluxes is required to maintain pump activity (Forgac, 1989; Blair et al., 1991).

Studies of ionic conductances in mammalian (Sims & Dixon, 1989) and avian osteoclasts (Ravesloot et al., 1989) as well as in related cell types, such as macrophages (Gallin & McKinney, 1988*a,b*), have revealed the presence of several distinct voltage- and $Ca^{2+}$-dependent $K^+$ conductances. Notable, in all of the above, is an inwardly rectifying potassium conductance. In addition, at least three different types of $K^+$ channels have now been reported in macrophages (for review *see* Gallin & McKinney, 1988*c*) and in chick osteoclasts (Ravesloot et al., 1989). Electrophysiological evidence for voltage-dependent $Ca^{2+}$ current has not been found in any of the above cells studied to date.

We have used patch-clamp techniques, both whole-cell and single-channel, to investigate the ionic currents of freshly isolated neonatal rabbit osteoclasts. We show that rabbit osteoclasts exhibit an inwardly rectifying conductance at negative potentials which is selective for $K^+$ and sensitive to $Ba^{2+}$. Inward $K^+$ current was the predominant current recorded in all cells in our study. In some cells, we also found an outwardly rectifying conductance at positive membrane potentials, which preliminary studies have shown to be an anion conductance (Kelly, Dixon & Sims, 1991). In this present study, we have characterized the ionic selectivity, voltage dependence and pharmacology of the macroscopic inwardly rectifying $K^+$ conductance in rabbit osteoclasts. In addition, we describe single-channel currents whose properties could account for the current

recorded in whole-cell configuration. We propose that inwardly rectifying $K^+$ current in rabbit osteoclasts provides a pathway capable of dissipating electrical potentials arising from electrogenic proton transport. A brief account of some of this work has appeared (Kelly et al., 1991).

## Materials and Methods

### Isolation of Osteoclasts

Osteoclasts were isolated from long bones of neonatal rabbits using methods similar to those described previously (Chambers et al., 1984). Briefly, the long bones of new-born New Zealand white rabbits were removed and placed in phosphate-buffered saline at room temperature. Bones were then scraped clean of adherent soft tissue and split longitudinally. The contents of the marrow cavities, containing osteoclasts and other cells, were curetted into Medium 199 (Gibco), buffered with HEPES and $HCO_3^-$ and supplemented with heat-inactivated fetal bovine serum (15%) and antibiotics. The marrow contents were further dispersed by repeated trituration using a pasteur pipette. Small aliquots (≈0.4 ml) of the resulting suspension were plated onto glass coverslips coated with collagen (Vitrogen 100, Collagen Corp., Palto Alto, CA) and incubated in 5% $CO_2$/95% air at 37°C for 60 min. Coverslips were then washed in phosphate-buffered saline to remove nonadherent cells and debris and then reincubated in fresh supplemented Medium 199 at 37°C for up to 16 hr. In some experiments, cells were stained for the presence of tartrate-resistant acid phosphatase using a histochemical staining kit (Cat. No. 387-A, Sigma).

### Electrophysiological Recording

Patch electrodes were pulled from 1.5-mm outside diameter and 1.1-mm inside diameter borosilicate glass tubing (Sutter Instrument) on a Brown Flaming P87 microelectrode puller. Electrodes had resistances of 2 to 6 MΩ when filled with intracellular solution. Electrodes were heat-polished and coated with beeswax to reduce capacitance. Seal resistances were in the range of 5 to 50 GΩ. Liquid junction potentials between the pipette and bath solutions were nulled before seals were made on cells. Junction potentials of 2 mV, between the bath and patch-clamp electrodes, were measured using a 3 M KCl agar bridge, and potentials shown here have been corrected.

In some experiments, perforated-patch recording techniques (Horn & Marty, 1988) were used. Nystatin (Sigma) was dissolved in dimethylsulphoxide (5 mg/ml) prior to dilution to a final concentration of 0.1 mg/ml in intracellular pipette solution. Pipette tips were first filled with nystatin-free solution and then back-filled with nystatin-containing solution. A gigaohm seal was then established on the cell and capacitance transients monitored. The capacitance of the cell was usually apparent within 10 min, with access resistance stabilizing at 10 to 15 MΩ within 20 min.

Currents were recorded with an Axopatch-1B amplifier (Axon Instruments), filtered with a 4-pole low-pass Bessel filter (−3 dB at 1 kHz) and digitized at a sampling frequency of 5 kHz using pClamp (Axon Instruments). Values of current and voltage reported in figures are averages of 10 to 50 points. Current records obtained with voltage-ramp commands were smoothed using a 4-point averaging routine that reduced the number of data points to facilitate display. A series resistance compensation of 80% was applied in most cases. Current and voltage were displayed on a Gould 3200S chart recorder and stored on computer disk as well as on video tape with a pulse-code modulator. All experiments were conducted at room temperature, 22–25°C. Cell capacitance values were obtained from the capacitance compensation circuitry on the amplifier or by integration of the uncompensated current transient (obtained using 10 mV voltage commands). Measures of series resistance ($R_{access}$) were obtained directly from the amplifier or calculated using the relationship $R_{access} = \tau/C$, where $C$ was obtained as described previously and $\tau$ was calculated by fitting of the uncompensated capacitance transient with a monoexponential function. Cells were considered acceptable for recording if they had a membrane potential of −70 mV or more negative and had an input resistance at depolarized potentials of ≥1 GΩ.

### Superfusion and Solutions

Coverslips with adherent osteoclasts were placed in a chamber mounted on an inverted microscope and superfused (1–2 ml/min) with physiological salt solution composed of (in mM): NaCl 130; KCl 5, $CaCl_2$ 1, $MgCl_2$ 1, HEPES 20, and glucose 10, adjusted to pH 7.4 with NaOH. Standard patch-clamp recording techniques were employed (Hamill et al., 1981). Electrode solution for both whole-cell and cell-attached recordings was normally composed of (in mM): KCl 140, $MgCl_2$ 1, HEPES 20, EGTA 1, and $CaCl_2$ 0.4, adjusted to pH 7.2 with KOH. Free [$Ca^{2+}$] was estimated to be ≈100 nM. In some cases, 0.5 mM ATP and 1 mM GTP were added to the standard electrode solution; however, no significant difference in membrane currents was noted when they were included. Extracellular $K^+$ concentration was altered by equimolar substitution of NaCl with KCl. In some experiments, 1 mM $Ba^{2+}$ was included in the extracellular solution to block $K^+$ current. In experiments investigating the time-dependent decrease of the whole-cell inward current at negative potentials, $Na^+$ was substituted with N-methyl-D-glucamine$^+$. Solution osmolarities were determined by freezing point depression ($\mu$ Osmette, Precision Instruments); values for extracellular solutions and for electrode-filling solutions were between 280–290 mOsm/liter.

## Results

### Osteoclast Identification

Osteoclasts were identified on the basis of their morphology, cytochemical staining and functional activity. Using phase-contrast optics, freshly isolated osteoclasts appeared flattened with multiple nuclei in an area of granular cytoplasm surrounded by pseudopodia (Fig. 1*A*). Such cells stained positive for tartrate-resistant acid phosphatase (Fig. 1*B*). When cells were incubated on slices of human dentine, resorption pits were formed (Fig. 1*C*). In addition, multinucleated cells retracted in response to calcitonin (*not shown*). By these criteria, the cells studied

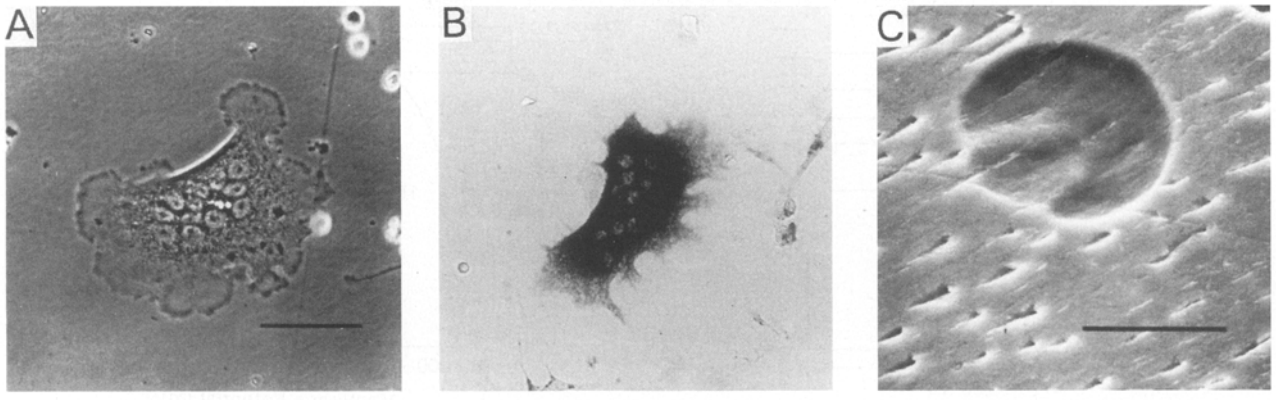


**Fig. 1.** Morphological and functional characteristics of isolated rabbit osteoclasts. (*A*) Phase-contrast light micrograph of an isolated rabbit osteoclast on collagen-coated substrate. Cell has 12 nuclei in an area of granular cytoplasm surrounded by pseudopodia. (*B*) Another osteoclast stained for tartrate-resistant acid phosphatase (dark regions represent staining). (*C*) Scanning electron micrograph of a resorption pit formed on a dentine slice following incubation for 24 hr at 37°C with freshly isolated osteoclasts. Cells were removed by washing, slices were then air dried and sputter coated prior to observation using a scanning electron microscope. Scale bar is 50 $\mu$m in each panel.

here were identified as osteoclasts (Vaes, 1988; Chambers, 1989).

### *I-V* Relation for Rabbit Osteoclasts

The whole-cell current-voltage relationship (*I-V*) determined under voltage-clamp showed inward rectification (Fig. 2). Cells were held at −62 mV and stepped from −102 to +38 mV in 20-mV increments. Hyperpolarizing commands elicited inward current (Fig. 2*A*), with little outward current apparent at more positive potentials. The *I-V* relation for the steady-state currents measured at 200 msec (boxes) is displayed in Fig. 2*B*. In addition, the continuous line joining the data points in Fig. 2*B* represents a voltage-ramp command from −122 to +48 mV at 85 mV/sec. The *I-V* obtained using the voltage ramp agrees well with steady-state values, and is therefore a valid measure of the steady-state *I-V* relation. The *I-V* measured is N-shaped, with more inward current obtained on hyperpolarization of the membrane from $E_K$ than outward current obtained in response to depolarizing commands. The *I-V* relation is shown at higher gain in the inset of Fig. 2*B*, where the current trace intersects the zero current level with a positive slope conductance at −78 mV, a value corresponding to the resting membrane potential of the cell recorded in current clamp. It is noteworthy that depolarizing commands from −62 to −22 mV resulted in apparent inward current (Fig. 2*A*). This is consistent with depolarization causing deactivation of the outward current active at the holding potential of −62 mV. This phenomenon gives rise to a region of negative slope between −62 and −22 mV on the *I-V* relationship (Fig. 2*B inset*). An inwardly rectifying *I-V* relation has also been reported for rat (Sims & Dixon, 1989) and chicken (Ravesloot et al., 1989) osteoclasts.

### The Inwardly Rectifying Current in Rabbit Osteoclasts is Selective for $K^+$

The selectivity of the inwardly rectifying current for potassium ions was investigated by varying the concentration of $K^+$ in the bathing solution ($[K^+]_{out}$). Membrane currents were measured using voltage-ramp commands and values for current reversal ($V_{REV}$) were determined as the potential at which the *I-V* relation intersected the zero current level. *I-V* relationships were first recorded in standard solutions containing 4.7 or 5 mM $K^+$ and then during superfusion with solutions in which $[K^+]_{out}$ was raised to 15, 47 and 120 mM. Increasing $[K^+]_{out}$ shifted the reversal potential, and the voltage around which the rectification occurred, positive along the voltage axis (Fig. 3*A*). The slope conductance of the *I-V* at negative potentials also increased as $[K^+]_{out}$ was increased. For example, in Fig. 3*A*, the slope conductance increased from 49 nS in 5 mM K solution to 69 and 138 nS in solutions containing 15 and 47 mM $K^+$, respectively. $V_{REV}$ was dependent on $[K^+]_{out}$ (Fig. 3*B*). The straight line in Fig. 3*B* is the least-squares best fit of the data and has a slope of 53 mV/10-fold change of $[K^+]_{out}$. This value is close to that predicted from the Nernst relation (59 mV/10-fold change in $[K^+]_{out}$) and suggests that the inward rectifier is largely selective for $K^+$.

Further evidence that the inwardly rectifying

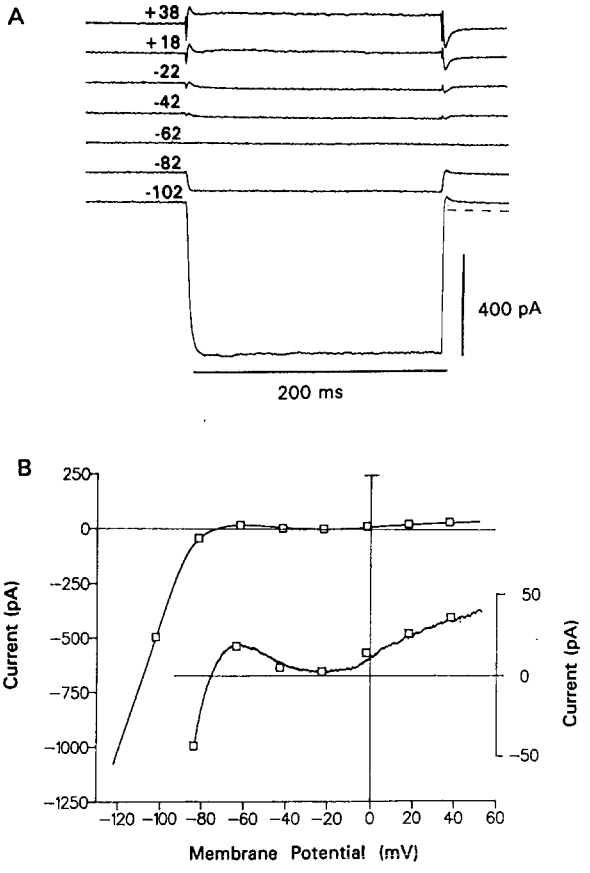


**Fig. 2.** Inwardly rectifying $K^+$ current in rabbit osteoclast. (*A*) Cell was held at −62 mV, and the membrane commanded to various potentials, as indicated to the left of the traces. Large inward currents were apparent in response to hyperpolarizing commands, indicative of inward rectification. At depolarizing potentials little outward current was activated. (*B*) The current-voltage relationship for the cell shown in *A*. Steady-state currents were measured at 200 msec (□). Continuous line is current elicited using a voltage-ramp command from −122 to 48 mV over 2 sec. The inset shows the *I-V* curve at a higher gain to reveal the negative slope region apparent between −65 and −10 mV. The cell capacitance was 76 pF.

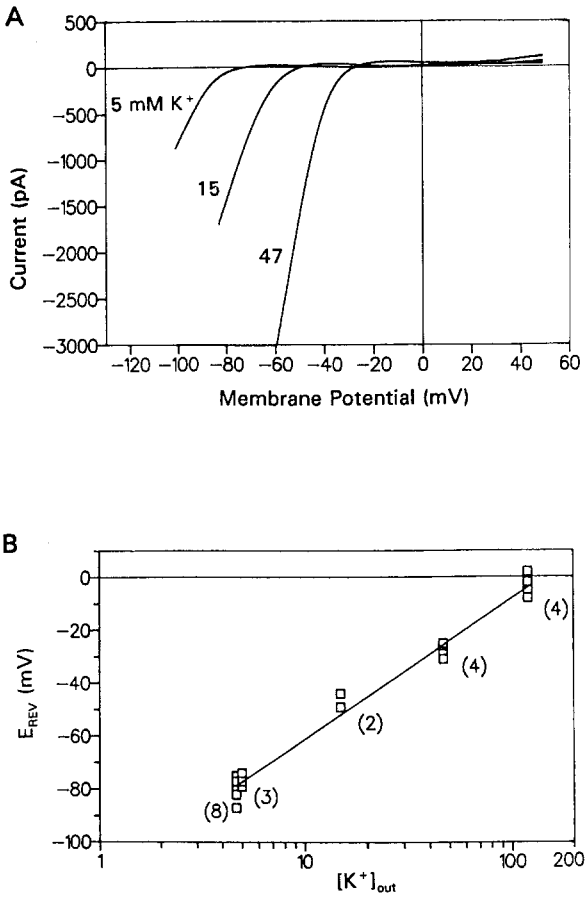


**Fig. 3.** Inward rectifier of osteoclasts is dependent upon $[K^+]_{out}$. *I-V* relationships were obtained using voltage-ramp commands from −120 to +50 mV over 2 sec. (*A*) External $K^+$ concentration was raised from 5 to 15 and 47 mM by path perfusion, shifting the reversal potential and the voltage around which rectification occurred positive along the voltage axis. The slope conductance (measured from the linear portion of the *I-V* at negative potentials) in 5, 15 and 47 mM $K^+$, was 49, 69 and 138 nS, respectively. (*B*) Zero current potentials ($V_{REV}$) for this and other cells are plotted as a function of $[K^+]_{out}$. The straight line is the least-squares best fit of the data, with a slope of 53 mV per 10-fold change of $[K^+]_{out}$. The number of cells studied is indicated in parentheses beside each data point. The capacitance of cell shown in *A* was 115 pF.

current is a $K^+$ current came from analysis of voltage- and time-dependent current relaxations. The membrane potential was stepped to −122 mV, to activate inward current, and then to more depolarized potentials to record current relaxations (Fig. 4). Ignoring early current recorded during settling of the clamp, the time course of decay of current relaxations was well fit with single exponentials. At potentials negative to $E_K$, outward current relaxations were elicited, with inward current relaxations at potentials positive to $E_K$. The reversal potential was obtained by interpolating between the two nearest points where the relaxations changed direction. In standard 5 mM $K^+$ bathing solution, the measured reversal potential was −77 ± 1 mV (mean ± SEM, $n$ = 6). When $[K^+]_{out}$ was raised to 47 mM, the current relaxations reversed at a more depolarized potential (−25 ± 3 mV, $n$ = 3). These values for reversal of the current relaxations are close to the $K^+$ equilibrium potential. Taken together, the evidence indicates that the inwardly rectifying current in rabbit osteoclasts is carried by $K^+$.

## Barium Blocks the Inward Rectifier

Barium has been demonstrated to block inwardly rectifying $K^+$ current in a variety of cells types

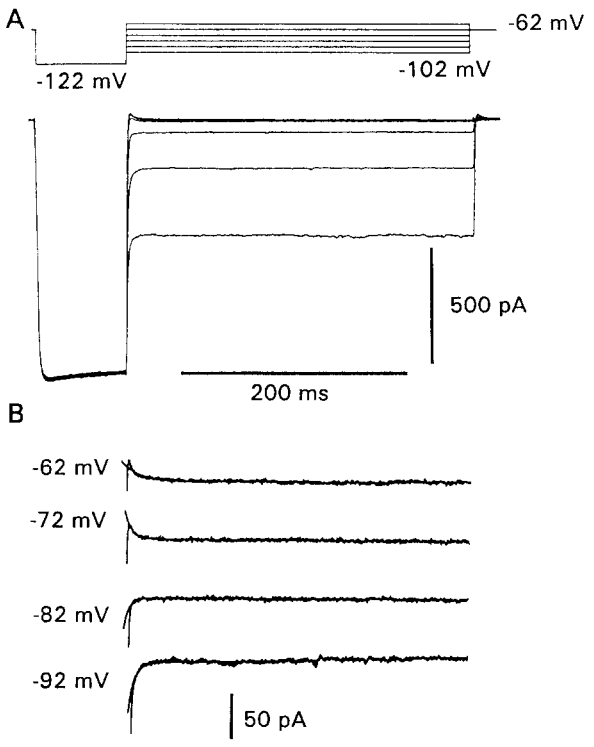


**Fig. 4.** Time-dependent decay of $K^+$ current. Cell was bathed in standard 5 mM $K^+$-containing salt solution. From a holding potential of −62 mV, the membrane was commanded to −122 mV, to activate inwardly rectifying $K^+$ current, and then stepped to various potentials, as indicated by the voltage commands at top. Currents are shown at higher gain in *B*, with test potentials shown to the left of the traces. Single exponential curves have been fit to the currents (lines through the data) and extrapolated back to the beginning of the voltage commands. Tail currents reversed direction at ≈ −78 mV, close to the predicted equilibrium potential for $K^+$. Time constants for the exponential curves are −62 mV, 6 msec; −72 mV, 6 msec; and −82 mV, 2 msec. Time constant for −92 mV was fixed at 4 msec to avoid fitting the current transient during settling of the clamp. Data are from the same cell as in Fig. 2.

(Standen & Stanfield, 1978; Sakmann & Trube, 1984; Gallin & McKinney, 1988*a*). We tested the effects of $Ba^{2+}$ on the macroscopic $K^+$ current recorded in rabbit osteoclasts. When whole-cell currents were recorded in standard extracellular bathing medium, the current records showed characteristic inwardly rectifying current with the *I-V* relationship crossing the zero current level at −76 mV and little outward current at positive potentials (Fig. 5*A*). Superfusion of the cell with extracellular solution containing 1 mM $Ba^{2+}$ reversibly blocked the inward current (Fig. 5*B*). Similar results were obtained in 10 other cells. The steady-state *I-V* relation for the cell, before and after $Ba^{2+}$, is shown in Fig. 5*C*. After barium, the inward current is blocked, leaving linear leak current (≈3 GΩ) which crosses the zero current level close to 0 mV. Figure 5*D* shows the difference current obtained by subtracting currents recorded in $Ba^{2+}$-containing solution from currents recorded in standard bathing solution. The difference current was inward at negative potentials, outward between −62 and −22 mV, and essentially zero at more positive potentials. We found no evidence for voltage-activated $Ca^{2+}$ current under these conditions. In addition, in seven cells recorded using the perforated-patch technique (Horn & Marty, 1988), which preserves the intracellular milieu, no voltage-activated inward $Ca^{2+}$ current was detected. Resting membrane potentials recorded in current-clamp mode with perforated-patch and conventional whole-cell recording were similar (−75 ± 2 mV, $n$ = 7 and −76 ± 2 mV, $n$ = 7, respectively), and inwardly rectifying $K^+$ current was present in all cells studied.

### Inactivation of the Inwardly Rectifying $K^+$ Current at Negative Potentials

It has been shown in a number of cell types that the time-dependent inactivation, or decay of the inwardly rectifying $K^+$ current at hyperpolarized potentials, is attributable, in part, to blockage by external $Na^+$ ions (Ohmori, 1978; Lindau & Fernandez, 1986; Gallin & McKinney, 1988*b*,*c*). In rabbit osteoclasts, we have also confirmed that the inward $K^+$ current exhibits pronounced inactivation at potentials hyperpolarized to −120 mV. To test whether the decay of the inward rectifier arose from blockage by external $Na^+$, we recorded currents in nominally $Na^+$-free solution (substituting N-methyl-D-glucamine$^+$ for $Na^+$ (Fig. 6)). In standard bathing solution, inactivation of the inwardly rectifying current was readily observed at potentials negative to −120 mV (Fig. 6*A*). When $Na^+$ was omitted from the extracellular bathing solution, the decay of the steady-state inward current at negative potentials was considerably reduced (Fig. 6*B*). Steady-state *I-V* relationships for the cell in Fig. 6*A* and *B* are shown in Fig. 6*C*, with current measured at 200 msec. Inactivation of the $K^+$ current in $Na^+$-containing solution gave rise to a region of negative slope between −140 and −170 mV. The steady-state *I-V* relation was essentially linear at negative potentials in $Na^+$-free solution. Similar findings were also observed in three other cells.

### Single-Channel Currents

The single-channel currents underlying the whole-cell currents were studied in the cell-attached patch configuration. When the recording pipette contained

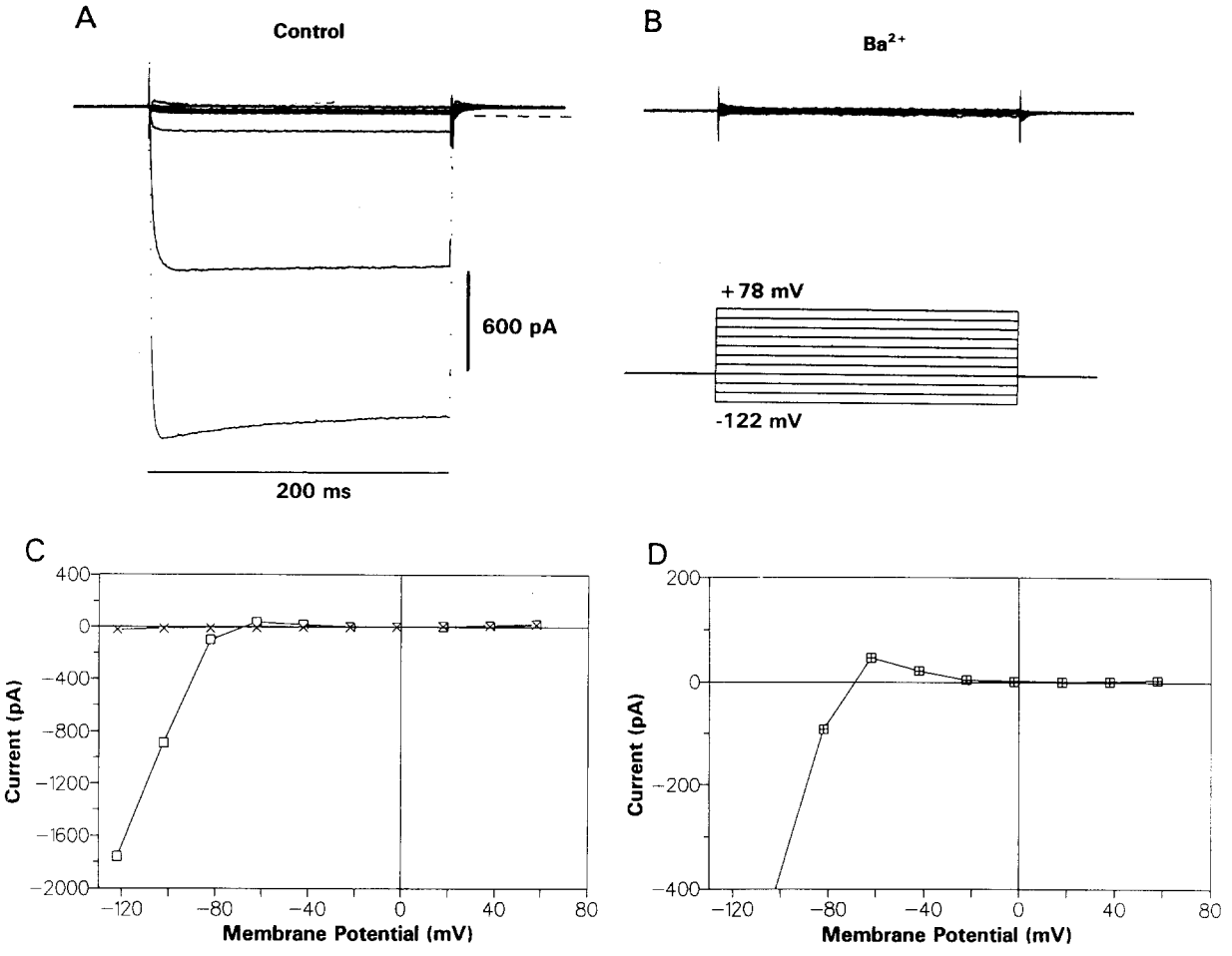


**Fig. 5.** Inwardly rectifying current is blocked by external barium. (*A*) Whole-cell currents were recorded in standard extracellular bathing solution. The membrane was stepped to −122 mV and then to +78 mV in 20 mV increments. Current records show characteristic inward $K^+$ current with no outward current apparent at positive potentials. (*B*) Superfusion of the cell with extracellular solution containing 1 mM $Ba^{2+}$ resulted in complete block of the inward current. (*C*) The steady-state *I-V* relation for the cell before (□) and after $Ba^{2+}$ (X) is shown. In $Ba^{2+}$ solution, the inward current is blocked leaving a small linear leak (≈3 GΩ), which crosses the zero current level between −20 and 0 mV. (*D*) The $Ba^{2+}$-sensitive difference current (⊞) is shown at higher gain, revealing that the $Ba^{2+}$ blocked current was inward at negative potentials, outward between −62 and −22 mV, and essentially zero at more positive potentials. Cell capacitance was 83 pF.

140 mM KCl, with 5 mM $K^+$ in the bath, single-channel events were observed at hyperpolarized potentials. Current amplitudes increased as the pipette potential became more positive (i.e., as the patch of membrane was hyperpolarized). No reversal of the currents was apparent (Fig. 7), indicating inward rectification of the unitary channel *I-V* relation. In patches that contained inward channel openings, from one to three channels were commonly observed. The slope conductance ($\gamma$) was determined from the slope of the linear portion of the *I-V* relation (Fig. 7*B*). For the cell shown in Fig. 7*A*, inward single-current events had a slope conductance of 26 pS with an estimated reversal between −60 and −70 mV (note that the ordinate in Fig. 7*B* is the *negative* of the pipette potential). The intercept of the single-channel current is close to the resting membrane potential (RMP) of −75 mV.

Variations in the resting potential of cells may have given rise to differences in the *I-V* relations measured in the cell-attached recording configuration. One way this was minimized was to zero the membrane potential by raising $[K^+]_{out}$ to 135 mM (where RMP was assumed to be close to 0 mV, *see* Fig. 8). In some cells, the single-channel conductance and $E_{REV}$ could be determined quickly using a voltage ramp. In cells shown in Fig. 8*A* and *B*, single-channel currents were measured in response to a

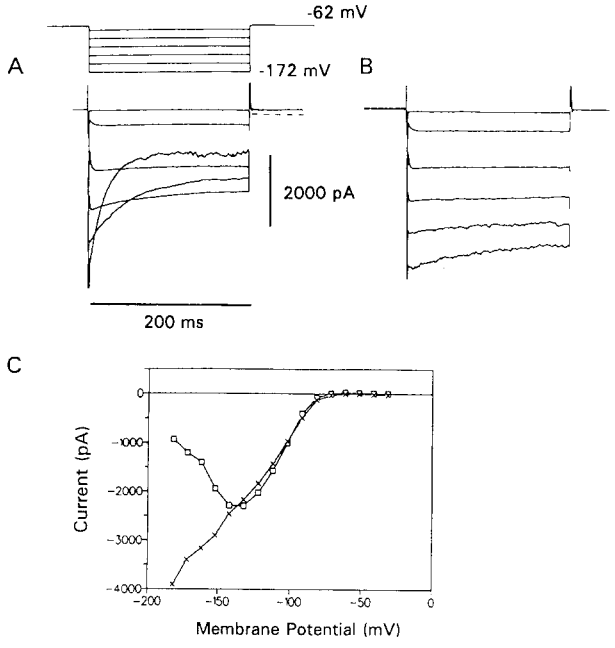


**Fig. 6.** Time-dependent decline of the inwardly rectifying current at negative potentials. (*A*) Whole-cell records from cell bathed in standard $Na^+$-containing solution. Cell was held at −62 mV and stepped from −172 to −72 mV in 20-mV increments. Dashed line indicates the zero current level. (*B*) Whole-cell current records from the same cell as in *A*, with N-methyl-D-glucamine$^+$ substituting for $Na^+$ in the bathing solution. Peak current after decay of the uncancelled portion of the membrane capacitance remained unchanged; however, steady-state "inactivation" has been largely removed in nominally $Na^+$-free bathing solution. (*C*) *I-V* relationship for the steady-state current as measured at 200 msec in $Na^+$-containing (□) and N-methyl-D-glucamine$^+$ (X) bathing solutions. Currents recorded in N-methyl-D-glucamine$^+$ solution were subtracted for a linear leak of 0.9 GΩ, which developed during recording. Cell capacitance was 110 pF.

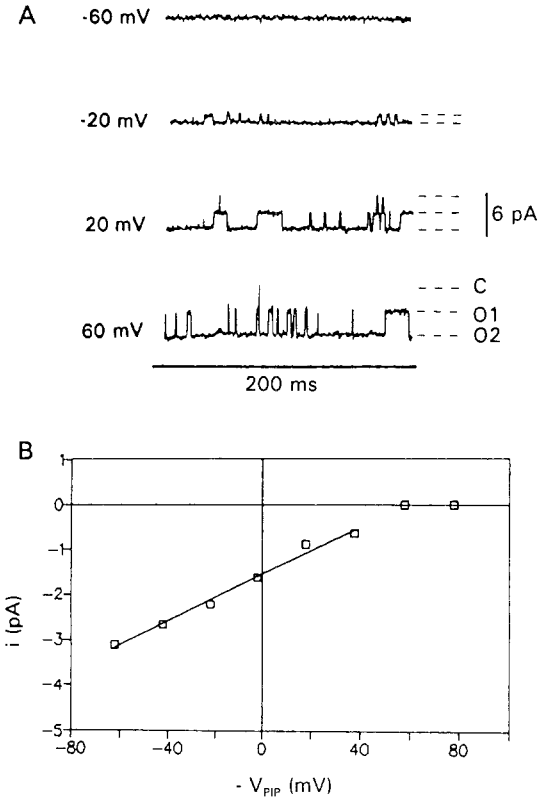


**Fig. 7.** Single-channel currents recorded from a rabbit osteoclast using the cell-attached configuration. (*A*) Inward currents, recorded with 140 mM $K^+$ in the recording pipette and standard $Na^+$ salt solution in the bath. Pipette potential ($V_{PIP}$) is shown to the left of each current trace. From 1 to 2 channels were open simultaneously in this patch, as indicated by the dashed lines at right of the current traces. Current was filtered (−3 dB) at 200 Hz and sampled at 1 kHz. (*B*) *I-V* relationship for channel activity shown in *A* is linear at negative potentials, with a slope conductance of 26 pS determined by linear least-squares best fit. Single-channel currents rectify around $E_K$, with no evidence of outward current.

ramp stimuli of −150 to +50 mV and $E_{REV}$ was determined as the voltage at which open- and closed-channel slopes intersected. Unitary conductance and $E_{REV}$ for inward single-channel currents recorded in the cell in Fig. 8*A*, with 140 mM $K^+$ in the pipette, was estimated to be 30 pS and −12 mV, respectively (mean $\gamma$ = 31 ± 1 pS, $n$ = 6). When $[K^+]$ was increased in the pipette from 140 to 200 mM, the conductance increased to 40 pS and the $E_{REV}$ shifted positive to +7 mV (mean $\gamma$ = 38 ± 1 pS, $n$ = 5). The shift in $E_{REV}$ observed upon increasing $[K^+]$ in the electrode from 140 to 200 mM is in the direction expected for a $K^+$-selective channel. Figure 8*C* shows a plot of single-channel conductance *versus* $[K^+]_{out}$ in double-logarithmic coordinates. Data are taken from ramp and steady-state measurements and fit by the equation $\gamma = C[K^+]_{out}^x$, where $C$ is a constant in pS, $[K^+]_{out}$ is in mM and $x$ was found to be 0.48. The exponent for dependence of $\gamma$ on $[K^+]_{out}$ agrees well with values reported for the inwardly rectifying $K^+$ channel in macrophages (Gallin & McKinney, 1988*a*,*b*) and rat basophilic leukemia cells (Lindau & Fernandez, 1986).

Inward single-channel events were not observed when $Ba^{2+}$ was applied to the extracellular surface of the membrane patch. In the cell displayed in Fig. 8*D*, the pipette tip was filled with 140 mM KCl and then backfilled with 140 mM KCl + 1 mM $Ba^{2+}$, with the bath containing standard 5 mM $K^+$ salt solution. At a pipette potential of 0 mV, inward single-channel fluctuations of 1.95 pA (28 pS assuming $E_K$ = 0 across the patch) were initially apparent but were abolished within 5 min of recording. In three other cells with 1 mM $Ba^{2+}$ in the recording pipette, single-

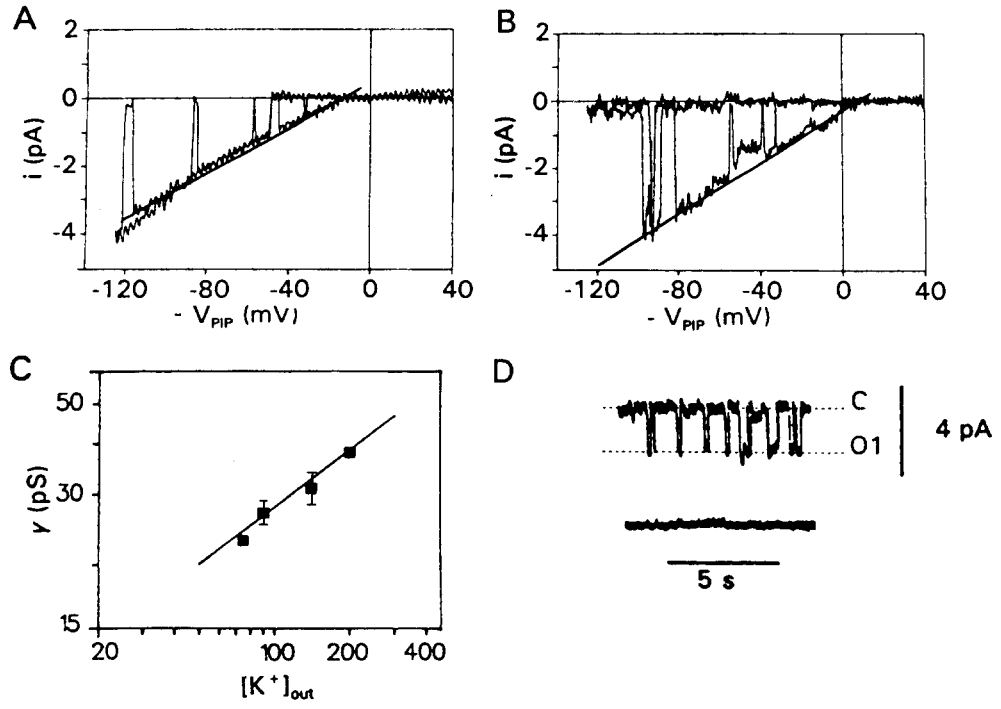


**Fig. 8.** Single-channel conductance and $E_{REV}$ are dependent on $[K^+]_{out}$. (*A*) *I-V* relationship for inward currents recorded in a cell-attached patch with a voltage ramp (150 mV/sec). Cell was bathed in 135 mM $K^+$ salt solution with 140 KCl in the recording electrode. A line has been drawn through the open current to the point at which open- and closed-channel states intersect ($E_{REV}$). The slope of the line was 30 pS. $E_{REV}$ was −11 mV. (*B*) *I-V* relationship from a different patch determined with a voltage ramp with 200 mM KCl in the electrode and 135 mM $K^-$ solution in the bath. Conductance was 40 pS, and channel fluctuations reversed at +7 mV. (*C*) Dependence of the single-channel conductance on the $K^+$ concentration in the pipette ($[K^+]_{out}$) in a double-logarithmic plot. Values shown are for $[K^+]_{out}$ = 75 mM ($n$ = 1); 90 mM ($n$ = 2); 140 mM ($n$ = 7); and 200 mM ($n$ = 5). The fitted line has a slope of 0.48. (*D*) Single-channel events recorded from a cell with 140 mM KCl and 1 mM $Ba^{2+}$ in the pipette and bathed in standard $Na^+$ solution. On initiation of recording, single-channel events of 1.9 pA were recorded at a $V_{PIP}$ = 0 mV (top trace), but after 5 min channel openings were not apparent (bottom trace). Records were filtered at 100 Hz and sampled at 1 kHz. Current traces in *A* and *B* were leak corrected by subtracting sweeps containing no channel openings.

channel events were no longer observed 5-10 min after initiation of recording.

## Discussion

In this present study, we used patch-clamp recording methods to investigate ionic currents in rabbit osteoclasts. Morphological, cytochemical and functional studies confirmed that the isolated cells described in this report are osteoclasts. Inwardly rectifying current was evident in all cells studied. We characterized the voltage dependence, ionic selectivity and pharmacology of the inward current. The inwardly rectifying current was found to be $K^+$ selective and sensitive to $Ba^{2+}$. The steady-state *I-V* relation for the inward $K^+$ current showed time-dependent inactivation at negative potentials which was largely removed in $Na^+$-free salt solution. Studies were undertaken to investigate the inwardly rectifying $K^+$ current at the single-channel level. Inward single-channel fluctuations were recorded, which did not reverse direction, were dependent on external $[K^+]$ and were sensitive to $Ba^{2+}$. Inwardly rectifying $K^+$ current has been described in osteoclasts from rat (Sims & Dixon, 1989) and chicken (Ravesloot et al., 1989). The present study extends these observations by characterizing the inward $K^+$ current in rabbit osteoclasts at the whole-cell and single-channel level. We found no evidence of other voltage-activated inward currents, such as $Ca^{2+}$ currents.

### Evidence for Inwardly Rectifying $K^+$ Current in Rabbit Osteoclasts

Evidence that the macroscopic inwardly rectifying current was a $K^+$ current was provided by experiments examining the voltage dependence, ionic selectivity and pharmacological blockage of the inward current. The macroscopic inward current was shown to be dependent on $[K^+]_{out}$, with the zero current potential shifting positive as $[K^+]_{out}$ was raised (Fig. 3). The dependence on $K^+$ was also confirmed in experiments investigating the time- and voltage-dependent decay of the macroscopic inward current

(Fig. 4). Current relaxations reversed direction with estimated reversal potentials close to the expected value for $E_K$. Moreover, reversal potentials shifted as expected for a $K^+$-selective channel when $[K^+]_{out}$ was increased. The presence of current relaxations suggests that time-dependent gating of the channel may contribute to the inward rectification we observed (Matsuda & Stanfield, 1989).

Barium, which has been shown to block inwardly rectifying $K^+$ currents in a variety of other cell types including rat (Sims & Dixon, 1989) and chicken osteoclasts (Ravesloot et al., 1989), eliminates the inward current in rabbit osteoclasts, leaving only residual leak current.

Time-dependent inactivation of steady-state inward current is a feature of the inward rectifier in a number of different preparations (Standen & Stanfield, 1978; Gallin & McKinney 1988*b*; Harvey & Ten Eick, 1988). Inactivation of whole-cell inward current was observed in rabbit osteoclasts at hyperpolarized potentials in standard $Na^+$-containing bathing solution, and the rate of inactivation increased at more negative potentials. When external $Na^+$ was replaced in the bathing solution with N-methyl-D-glucamine$^+$, inactivation was no longer observed and the steady-state current at negative potentials exhibited a linear *I-V* relation (Fig. 5). $Na^+$-dependent inactivation of the inward rectifier has been described in detail in tunicate egg (Ohmori, 1978) and frog skeletal muscle (Standen & Stanfield, 1978) and has been attributed to low-affinity block of the $K^+$ channel by $Na^+$. Time-dependent inactivation, attributable in part to $Na^+$, has also been reported at the whole-cell and single-channel level in mouse (Gallin & McKinney, 1988*a*) and human (Gallin & McKinney, 1988*b*) macrophages.

## Single-Channel Currents with Properties of the Macroscopic Inward Rectifier

Inward single-channel currents were recorded in cell-attached patches (Figs. 7 and 8). Single-channel currents reversed around $E_K$ and had an estimated single-channel conductance of 31 pS. The unitary conductance was dependent on external $K^+$, being approximately proportional to the square root of $[K^+]_{out}$. Furthermore, the reversal potential for the inward currents shifted positive when $[K^+]_{out}$ was raised, as expected for a channel selective for $K^+$ (Fig. 8). Inward single-channel events were also blocked by $Ba^{2+}$, providing further evidence that inward single-channel currents in rabbit osteoclasts underlie the macroscopic inwardly rectifying $K^+$ current. Inwardly rectifying $K^+$ channels of 25 pS were described recently in rat osteoclasts (Sims et al., 1991).

## Comparison with Other Cell Types

Inwardly rectifying $K^+$ current has been described in a number of cells, including skeletal (Standen & Stanfield, 1978) and cardiac muscle cells (Sakmann & Trube, 1984; Harvey & Ten Eick, 1988; Matsuda & Stanfield, 1989) starfish egg cells (Hagiwara & Jaffe, 1979), human malignant glioma cells (Brismar & Collins, 1989), rat basophilic leukemia cells (Lindau & Fernandez, 1986) and macrophages (Gallin & McKinney, 1988*a,b,c*, 1989). The characteristics of the inward rectification described in these previous studies appear similar to the properties of the inwardly rectifying $K^+$ current of rabbit osteoclasts. Macroscopic steady-state inwardly rectifying current in the mouse J774.1 macrophage cell line (Gallin & McKinney, 1988*a*), as well as cardiac ventricular myocytes (Harvey & Ten Eick, 1988), exhibited inactivation at negative potentials which was decreased by the removal of extracellular $Na^+$. Inward current in macrophages was dependent on $[K^+]_{out}$ and sensitive to pharamacological blockers such as $Ba^{2+}$ and $Cs^+$ (Gallin & McKinney, 1988*a,b*; Harvey & Ten Eick, 1988).

Unitary conductances reported for macrophages (Gallin & McKinney, 1988*a*) and ventricular myocytes (Sakmann & Trube, 1984) are in the range of 27 to 29 pS, which is close to the unitary conductance of the channels recorded in rabbit osteoclasts (31 pS). Although voltage-dependent inactivation of single-channel currents in rabbit osteoclasts was not investigated, inactivation was shown to be a property of the mouse J774.1 macrophage cell line (Gallin & McKinney, 1988*a*). Thus, in these respects (*I-V* relations, dependence on $[K^+]_{out}$ and sensitivity to $Ba^{2+}$ blockage), the inward single-channel currents seen in rabbit osteoclasts resemble those described in macrophages.

Similarities in the electrophysiological properties of osteoclasts and macrophages are not unexpected, since it appears that these cells share many common properties (for review *see* Chambers, 1989). Both osteoclasts and macrophages originate from hematopoietic tissue and display antigenic similarities. In addition, like macrophages, osteoclasts are capable of phagocytosis. However, despite these similarities, osteoclasts exhibit several distinct characteristics which are not shared by macrophages. These include calcitonin responsiveness and the ability to resorb bone extracellularly. These criteria (calcitonin responsiveness and the ability to excavate bone) together with multinuclearity and the development of a highly specialized "ruffled border," distinguish osteoclasts both functionally and morphologically from mononuclear phagocytic cells.

### Other Currents

The inwardly rectifying $K^+$ current was the major current recorded in all rabbit osteoclasts under the above conditions. In 30–40% of cells, outwardly rectifying current was also apparent (M. Kelly, J. Dixon and S. Sims, *in preparation*). Other than $K^+$ current, no evidence for voltage-activated inward currents, such as $Ca^{2+}$ currents, was found. An absence of voltage-gated $Ca^{2+}$ current has also been noted in rat (Sims & Dixon, 1989) and chicken osteoclasts (Ravesloot et al., 1989) as well as in macrophages (Gallin & McKinney, 1988*a,b*). However, since our experiments in rabbit osteoclasts have not investigated the presence of voltage-gated $Ca^{2+}$ current under conditions specifically designed to favor identification, we cannot eliminate the possibility that $Ca^{2+}$ channels are present in low density in these cells. It is also possible that dialysis of the cytoplasm with the electrode solution may result in "wash-out" of those currents that require a specific intracellular milieu. However, this is unlikely since experiments with nystatin perforated-patch recording yielded similar results. Alternatively, the presence of $Ca^{2+}$ channels in osteoclasts may depend on culture conditions or cell-substrate interactions (Miyauchi et al., 1990), which may not be present when acutely isolated cells are plated on collagen-coated glass substrate. In contrast to what we have found in osteoclasts, voltage-gated $Ca^{2+}$ currents have been demonstrated in osteoblastic cells (Chesnoy-Marchais & Fritsch, 1988; Caffrey & Farach-Carson, 1989; Guggino et al., 1989).

### Function of Inwardly Rectifying $K^+$ Current in Osteoclasts

We have demonstrated that the predominant conductance in freshly isolated rabbit osteoclasts is an inwardly rectifying $K^+$ conductance. When $K^+$ conductance was blocked by $Ba^{2+}$, cells depolarized from $\approx -75$ mV to around 0 mV, indicating that inwardly rectifying $K^+$ current sets the resting membrane potential of rabbit osteoclasts. A similar function has been attributed to the inward rectifier of rat basophilic leukemia cells (Lindau & Fernandez, 1986).

Osteoclastic bone resorption involves the secretion of enzymes and the transport of $H^+$ ions into the resorption lacuna. Recent evidence has revealed that acidification of the resorption lacuna is mediated by the vacuolar class of ATP-driven proton pump (Blair et al., 1989; Bekker & Gay, 1990; Väänänen et al., 1990), which is electrogenic (Forgac, 1989). Thus, movement of counterions is required to dissipate charge accumulation arising from the transport of $H^+$ across the osteoclast ruffled border. The inwardly rectifying $K^+$ current provides such a conductive pathway. Electrogenic $H^+$ transport would hyperpolarize the cell, activating inward $K^+$ current, which in turn would act to prevent excessive hyperpolarization by clamping the membrane at $E_K$. At depolarized potentials, the channels would close, minimizing efflux of $K^+$.

In conclusion, we have demonstrated that inwardly rectifying $K^+$ current is the predominant conductance in rabbit osteoclasts. Our studies have provided evidence for single channels whose properties could give rise to the macroscopic inwardly rectifying $K^+$ current. We have found no evidence for other voltage-dependent inward currents in these cells, but outwardly rectifying current, previously reported to be $Cl^-$ current, was noted in some cells (Kelly et al., 1991). The membrane properties of rabbit osteoclasts are similar to those described in another mammalian species, rat (Sims & Dixon, 1989). The presence of common characteristics among different mammalian species suggests that these ionic conductances play important roles in osteoclast function and regulation.

This work was supported by The Arthritis Society and the Medical Research Council of Canada. M.E.M.K. was supported by a fellowship, S.J.D. a development Grant and S.M.S. a scholarship from the Medical Research Council. We thank Dr. Zu Gang Zheng for help with scanning microscopy.

## References

Baron, R., Neff, L., Louvard, D., Courtoy, P.J. 1985. Cell-mediated extracellular acidification and bone resorption: Evidence for a low pH in resorbing lacunae and localization of a 100-kD lysosomal membrane protein at the osteoclast ruffled border. *J. Cell Biol.* **101:**2210–2222

Bekker, P.J., Gay, C.V. 1990. Biochemical characterization of an electrogenic vacuolar proton pump in purified chicken osteoclast plasma membrane vesicles. *J. Bone Mineral Res.* **5:**569–579

Blair, H.C., Kahn, A.J., Crouch, E.C., Jeffrey, J.J., Teitelbaum, S.L. 1986. Isolated osteoclasts resorb the organic and inorganic components of bone. *J. Cell Biol.* **102:**1164–1172

Blair, H.C., Teitelbaum, S.L., Ghiselli, R., Gluck, S. 1989. Osteoclastic bone resorption by a polarized vacuolar proton pump. *Science* **245:**855–857

Blair, H.C., Teitelbaum, S.L., Tan, H., Koziol, C.M., Schlesinger, P.H. 1991. Passive chloride permeability charge coupled to $H^+$-ATPase of avian osteoclast ruffled membrane. *Am. J. Physiol.* **260:**C1315–1324

Brismar, T., Collins, V.P. 1989. Inwardly rectifying potassium channels in human malignant glioma cells. *Brain Res.* **480:**249–258

Caffrey, J.M., Farach-Carson, M.C. 1989. Vitamin $D_3$ metabolites modulate dihydropyridine-sensitive calcium currents in clonal rat osteosarcoma cells. *J. Biol. Chem.* **264:**20265–20274

Chambers, T.J. 1989. The origin of the osteoclast. *Bone Mineral Res.* **6:**1–25

Chambers, T.J., Revell, P.A., Fuller, K., Athanasou, N.A. 1984.

Resorption of bone by isolated rabbit osteoclasts. *J. Cell Sci.* **66**:383–399

Chesnoy-Marchais, D., Fritsch, J. 1988. Voltage-gated sodium and calcium currents in rat osteoblasts. *J. Physiol.* **393**:291–311

Forgac, M. 1989. Structure and function of vacuolar class of ATP-driven proton pumps. *Physiol. Rev.* **69**:765–796

Gallin, E.K., McKinney, L.C. 1988*a*. Inwardly rectifying whole-cell and single-channel K currents in the murine macrophage cell line J774.1. *J. Membrane Biol.* **103**:41–53

Gallin, E.K., McKinney, L.C. 1988*b*. Patch-clamp studies in human macrophages: Single-channel and whole-cell characterization of two $K^+$ conductances. *J. Membrane Biol.* **103**:55–66

Gallin, E.K., McKinney, L.C. 1988*c*. Potassium conductances in macrophages. *In:* Cell Physiology of Blood. R.B. Gunn, and J.C. Parker, editors. pp. 315–332. Rockefeller University Press, New York

Gallin, E.K., McKinney, L.C. 1989. Ion transport in Phagocytes. *In:* The Neutrophil: Cellular Biochemistry and Physiology. M.B. Hallet, editor. pp. 243–259. CRC Press, Boca Raton (FL)

Guggino, S.E., Lajeunesse, D., Wagner, J.A., Snyder, S.H. 1989. Bone remodeling signaled by a dihydropyridine- and phenylakylamine-sensitive calcium channel. *Proc. Natl. Acad. Sci.* USA **86**:2957–2960

Hagiwara, S., Jaffe, L.A. 1979. Electrical properties of egg cell membranes. *Annu. Rev. Biophys. Bioeng.* **8**:385–416

Hamill, O.P., Marty, A., Neher, E., Sakmann, B., Sigworth, F.J. 1981. Improved patch-clamp techniques for high-resolution current recordings from cells and cell-free membrane patches. *Pfluegers Arch.* **391**:85–100

Harvey, R.D., Ten Eick, R.E. 1988. Characterization of the inward rectifier potassium current in cat ventricular myocytes. *J. Gen. Physiol.* **91**:593–615

Horn, R., Marty, A. 1988. Muscarinic activation of ionic currents measured by a new whole-cell recording method. *J. Gen. Physiol.* **92**:145–159

Kelly, M.E.M., Dixon, S.J., Sims, S.M. 1991. Potassium and anion currents in rabbit osteoclasts. *Biophys. J.* **59**:461*a*

Lindau, M., Fernandez, J.M. 1986. A patch-clamp study of histamine-secreting cells. *J. Gen. Physiol.* **88**:349–368

Matsuda, H., Stanfield, P.R. 1989. Single inwardly rectifying potassium channels in cultured muscle cells from rat and mouse. *J. Physiol.* **414**:111–124

Miyauchi, A., Hruska, K.A., Greenfield, E., Duncan R., Alvarez, J., Barattolo, R., Colucci, S., Zambonin-Zallone, A., Teitelbaum, S.L., Teti, A. (1990). Osteoclast cytosolic calcium, regulated by voltage-gated calcium channels and extracellular calcium, controls podosome assembly and bone resorption. *J. Cell Biol.* **111**:2543–2552

Ohmori, H. 1978. Inactivation and steady-state current noise in the anomalous rectifier of tunicate egg cell membrane. *J. Physiol.* **281**:77–99

Ravesloot, J.H., Ypey, D.L., Vrijheid-Lammers, T., Nijweide, P.J. 1989. Voltage-activated $K^+$ conductances in freshly isolated embryonic chicken osteoclasts. *Proc. Natl. Acad. Sci. USA* **86**:6821–6825

Sakmann, B., Trube, G. 1984. Conductance properties of single inwardly rectifying potassium channels in ventricular cells from guinea-pig heart. *J. Physiol.* **347**:641–657

Sims, S.M., Dixon, S.J. 1989. Inwardly rectifying $K^+$ current in osteoclasts. *Am. J. Physiol.* **256**:C1277–C1282

Sims, S.M., Kelly, M.E.M., Dixon, S.J. 1991. $K^+$ and $Cl^-$ currents in freshly isolated rat osteoclasts, *Pfluegers Arch.* **419**:358–370

Standen, N.B., Stanfield, P.R. 1978. A potential- and time-dependent blockage of inward rectification in frog skeletal muscle fibres by barium and strontium ions. *J. Physiol.* **280**:169–191

Väänänen, H.K., Karhukorpi, E.-K., Sundquist, K., Wallmark, B., Roininen, I., Hentunen, T., Tuukkanen, J., Lakkakorpi, P. 1990. Evidence for the presence of a proton pump of the vacuolar $H^+$-ATPase type in the ruffled borders of osteoclasts. *J. Cell Biol.* **111**:1305–1311

Vaes, G. 1988. Cellular biology and biochemical mechanism of bone resorption. A review of recent developments on the formation, activation, and mode of action of osteoclasts. *Clin. Orthop.* **231**:239–271